A Heat-Transfer Rate Inducing System (H-TRIS) Test Method

Citation for published version:
Maluk, C, Bisby, L, Krajcovic, M & Torero, JL 2016, 'A Heat-Transfer Rate Inducing System (H-TRIS) Test Method', *Fire Safety Journal*. https://doi.org/10.1016/j.firesaf.2016.05.001

Digital Object Identifier (DOI):
10.1016/j.firesaf.2016.05.001

Document Version:
Peer reviewed version

Published In:
Fire Safety Journal

A Heat-Transfer Rate Inducing System (H-TRIS) Test Method

Cristian Maluk[1,2,*], Luke Bisby[1], Michal Krajcovic[1], and Jose Luis Torero[2]

[1] School of Engineering, The University of Edinburgh, UK

[2] School of Civil Engineering, The University of Queensland, Australia

ABSTRACT

A novel fire testing method, named the Heat-Transfer Rate Inducing System (H-TRIS), is presented and described in this paper. The method directly controls the thermal boundary conditions imposed on a test specimen by controlling a specified time-history of incident radiant heat flux at its exposed surface. Accounting for the absorptivity and thermal losses at the exposed surface of the test specimen, H-TRIS can be programmed to control the net heat flux at the exposed surface; thus controlling the in-depth time dependent temperature distributions within the test specimen. H-TRIS can be used for imposing a wide range of time-histories of incident radiant heat flux (e.g. constant, linear, stepped), or in-depth time dependent temperature distributions (i.e. specified thermal gradients). Notably, this enables simulation of thermal boundary conditions experienced by materials or structures exposed to any source of heat – during a conventional fire test (e.g. standard furnace test), a large-scale fire test, a real fire, or some other thermal boundary conditions calculated using a fire model (e.g. zone or computational fluid dynamics model). H-TRIS enables complementary experimental studies with excellent repeatability at comparatively low economic and temporal costs relative to traditional furnace test methods, thus permitting multiple repeat tests and statistical studies of response to heating. Application of H-TRIS within a research project studying heat-induced concrete spalling is briefly presented and discussed, to illustrate the significance and novelty of the new fire testing method.

KEYWORDS: Fire testing, H-TRIS, thermal boundary conditions, heat flux, fire safe design, heat-induced concrete spalling.

[*] Corresponding Author:

Address: School of Civil Engineering, The University of Queensland, Brisbane QLD 4072, Australia.

Email: c.maluk@uq.edu.au

Tel: +61 7 3365 3518

1 INTRODUCTION AND BACKGROUND

This paper presents a novel fire test method, named the Heat-Transfer Rate Inducing System (H-TRIS), which directly controls the thermal boundary conditions imposed on a test specimen by controlling a specified time-history of incident radiant heat flux at its exposed surface. This approach to fire testing of structural materials supports a philosophical departure from conventional furnace testing to define fire resistance.

The fire safe design of structural systems has historically been based on the concept of compliance with standard fire test standards [1]. At present, fire safe structural performance is typically (but not always [2]) defined by specifying a time of standard heating for which a structural element (or system) can 'survive' a 'severe' compartment fire. The term 'survive' is often defined in terms of exceeding a critical value of some specific variable (e.g. temperature, deflection). The introductory section of this paper provides a background discussion to demonstrate the novelty and significance of the proposed test method, and is divided into two thematic segments in which (1) fire safe structural design and (2) fire testing of structures and structural materials are examined.

1.1 Fire Safe Structural Design

Findings derived from studies on full-scale tests and from real fire events have shown that structural failures during or after fire, while rare, are often governed by heat-induced forces and relative thermal deformations between elements in a structural system [3, 4, 5, 6]. There is therefore a growing need for physics-based 'first principles' tools for the fire safe design of structures [7] to permit structural fire safety design considering 'full frame' structural response.

The fire safe design of building structures has historically been based on demonstrating compliance with standard fire testing procedures and ratings, wherein the design of individual structural elements is required to comply with prescribed design criteria to achieve specific fire resistance ratings when subjected to a standard fire [8]. In circumstances where a particular design cannot be evaluated using the prescribed criteria, or if potential gains can be realized (e.g. structural optimization, cost savings, or architectural freedom) by a more rigorous assessment, a performance based full frame structural fire safety design approach may be taken. In such cases, the performance of the structure during and after fire is quantitatively evaluated, aiming to demonstrate 'acceptability' according to a range of performance criteria, or in some cases by demonstrating equivalence to an acceptable, deemed-to-satisfy design solution. Performance based full frame structural fire safety design is rightly becoming increasingly common [9, 10, 11].

In practice, structural performance during fire is typically assessed following three steps [12, 13]: (1) definition of the design fire(s) to describe a range of credible fire scenarios, (2) analysis of the thermal boundary conditions and heat transfer between the fire(s) and the structural element(s), and (3) calculation of the thermal and mechanical response of the structural elements (or ideally, in the most advanced cases, structural systems) to assure appropriate levels of structural stability and compartmentation.

Design Fires

In the fire safe design of structures, the design fire(s) should represent the range of credible scenarios necessary to evaluate the performance of the structural element (or structure), whilst attempting to adequately account for the possible influences of the temporal and spatial evolution of a potential fire; but without generating spurious complexity given the large number of unknowns and infinite number of potential fire events. Commonly prescribed structural design fires used around the world are defined by gas phase time-temperature curves (i.e. time-histories of temperatures inside a fire compartment) (see Figure 1), typically assume homogenous conditions inside a fire compartment [14, 15], and have in many cases been semi-arbitrarily defined (e.g. [16]).

Coined in the 1970s, the term *natural fires* [17] was originally intended to describe alternative design fire scenarios that could be used for steel-framed buildings [18, 19]. The *natural fire* concept allowed calculation of more physically realistic time-temperature curves based on the specific ventilation, fuel type/amount, and interior lining materials in a given compartment.

A central assumption in the standard and natural fire concepts is that uniform burning, and therefore uniform temperature distribution inside the fire compartment, results in the worst case scenario for structural performance. This last has been scrutinized by several authors (e.g. [20, 21]) and found to be wanting in some cases; such fires do not *necessarily* represent the worst case for full structure response in real fires. As a result, researchers and designers have recently focused their efforts on defining temporally and spatially non-uniform (e.g. travelling) design fires [22, 23, 24].

Despite advances in understanding fully developed compartment fires (e.g. [21, 25, 26, 27, 28]), within the structural fire safety engineering community design fires remain almost exclusively defined by (or by equivalence to) standard (or in some cases *natural* or *parametric*) gas phase time-temperature curves [29].

Thermal Boundary Conditions

To understand the need for the novel fire testing approach described in the current paper, a brief review of heat transfer theory is required in this section. Regardless of the design fire selected, the heat transferred from the 'fire' to the exposed surfaces of a structure is normally expressed in terms of a net heat flux, $\dot{q}''_{net}$ [30]:

$$\dot{q}''_{net} = -k_s \frac{\partial T}{\partial x}\bigg|_{x=0} \quad (1)$$

Where k_s is the thermal conductivity of the solid, and $\frac{\partial T}{\partial x}\big|_{x=0}$ represents the in-depth time dependent temperature distribution at the exposed surface. For simplicity, in the current analysis heat conduction through the surface is taken only in the direction of the principal heat flow. If the design fire is defined by a time-history of gas temperatures inside a fire compartment, simplified calculations can be used to correlate the gas temperature (T_g) with the net heat flux at the exposed surface of structure by considering heat transfer by radiation and convection, thus:

$$h_c(T_g - T_s) + F_{g,s}\varepsilon_g\sigma T_g^4 - \alpha_s\sigma T_s^4 = \dot{q}''_{net} \quad (2)$$

Where T_s is the exposed surface temperature of the solid element (i.e. structural element). The absorptivity at the exposed surface and the emissivity of the gases inside the compartment are given by α_s and ε_g, respectively. The Stefan-Boltzmann constant, σ, and an average convective heat transfer coefficient, h_c, are used to describe heat transferred towards the exposed surface of the structural element by radiation and convection, respectively. It is noteworthy that the formulation presented in Equation 2 assumes that the convection and radiation modes of heat transfer at the exposed surface are functions of a single gas temperature (T_g). This assumption is acceptable for characterizing the boundary conditions during a fully developed compartment fire, where the radiation field may be considered to be in thermal equilibrium within the compartment; i.e. there is no radiation exchange between the gas phase and the boundaries of the compartment, and thus gas temperatures can be used to establish radiative heat fluxes [31]. The view factor for radiation heat transfer between the gas and the exposed surface of the structural element, $F_{g,s}$, is generally assumed as unity [30]. Under certain conditions, the absorptivity of the exposed surface and emissivity of the gases may be considered equal [30]; hence it can be considered that there is an *equivalent* fire emissivity (ε_f). Equation 2 may then be simplified as:

$$h_c\left(T_g - T_s\right) + \varepsilon_f \, \sigma \left(T_g^4 - T_s^4\right) = \dot{q}''_{net} \tag{3}$$

On the basis of Equations 2 or 3, the thermal boundary conditions can be described using a single time-temperature curve, along with an assumption that variations in thermal conditions at the surface of the structural element (i.e. absorptivity, emissivity, and convective heat transfer coefficient) are not significant.

Structural Fire Behaviour

Once the thermal boundary conditions are defined, the heat transfer problem can be treated using a heat conduction model (refer to Equation 1) which yields the in-depth time-dependent temperature distribution within a structural element. Mechanical strains due to applied loading and restrained thermal expansion can then be determined by considering temperature dependent constituent material mechanical properties.

The complexity of existing analysis methods for structures in fire varies significantly; this can be as simple as designing based on a critical temperature criterion for structural elements considered in isolation, or as complex as considering full structural behaviour of a structural system during and potentially after fire [12].

1.2 Fire Testing of Materials and Structures

During the late 19th Century, an era of rapid innovation in building design brought on by novel structural materials and systems along with efforts to save space and build higher, led to the development of the concept of "fire-resistant" construction [32, 33]. So-called *"fire and water"* tests became common practice for manufacturers of emerging fire resisting structural materials and systems. Attempts were made to advertise new products' and systems' *fire proof* characteristics using various means of demonstration [34]; however this approach soon became untenable due to the variability of demonstration techniques used.

By the turn of the 20th Century, efforts were made by both American and European testing organizations, along with other stakeholders in the building construction community, to define a uniform standard fire resistance test known today as the "standard furnace test" [34, 35, 36, 37, 38]. In the United States, a standard time-temperature curve was first proposed at the 1917 NFPA annual meeting [16]. The actual source data behind the selected curve is unknown to the authors. Nonetheless, since first being adopted in 1918 [39], this standard time-temperature curve (or similar curves used around the world) has remained essentially unchanged, and is now widely used not only in contemporary fire resistance testing, but also sometimes as a design fire or a deemed-to-satisfy comparator in performance-based structural fire safety engineering design [29, 40]. Presently there are a wide range of prescribed time-temperature curves available for use as potential design fire scenarios in various applications (see Figure 1), including: cellulosic (often referred to as the standard fire) [29], hydrocarbon [41], modified-hydrocarbon [42], RWS

(*Rijkswaterstaat*) [43], RABT-ZTV (railways or highways) [44], external exposure [41], and slow-heating (or smouldering) [41], among others.

During the 20th Century, the establishment of government and private experimental testing facilities with appropriate equipment, credentials, and impartiality, led to a regulatory environment in which testing facilities could systematically test building materials and structural elements under 'standard' conditions based on these time-temperature curves, initially for the purposes of comparative testing only. With an agreed standard fire resistance testing methodology, subsequent decades saw considerable growth of the fire resistance testing community in the number and cost of standard fire testing facilities worldwide. Recognizing clear inconsistencies of thermal exposures amongst different fire testing furnaces, in recent decades efforts have been aimed at standardizing fire testing furnaces and procedures; for instance by regulating the furnace lining materials [45], the gauges used to control and measure the furnace temperature [46], and the pressure and oxygen levels inside the furnace chamber [47].

Considerable differences in the design, construction and operation of fire resistance testing furnaces remain (e.g. furnace dimensions, lining materials, the positions of burner outlets, procedures to control the burner operation, fuel type, gauge for temperature control), however with some standardization of their construction and operation [48]. It appears that the design of furnaces remains largely based on past experience of individual furnace manufacturers.

The use of standard time-temperature curves and fire testing furnaces have become foundational principles of testing structural elements for regulatory compliance, but also for research and development within the structural fire engineering research community. Within the research community, experimental in-depth temperature distributions are widely used to validate material thermal properties and heat transfer models (e.g. [8]). Such work sometimes overlooks the complexities associated with the thermal boundary conditions experienced during a standard fire resistance test (or a real fire). Possibly for this reason, the oil and gas fire safety industries generally define boundary conditions in fire in terms of heat fluxes rather than furnace temperatures [49]. The notion that a standard time-temperature curve imposed on a structural element in a furnace can replicate a credible worst case fire, and further that it standardises the thermal exposure experienced by the full range of construction materials (e.g. concrete, steel, timber) is at the heart of contemporary fire testing of structures and structural materials; notwithstanding admirable recent work in Europe to harmonize testing performed in different furnaces, there remains doubt regarding both claims [7, 14, 50].

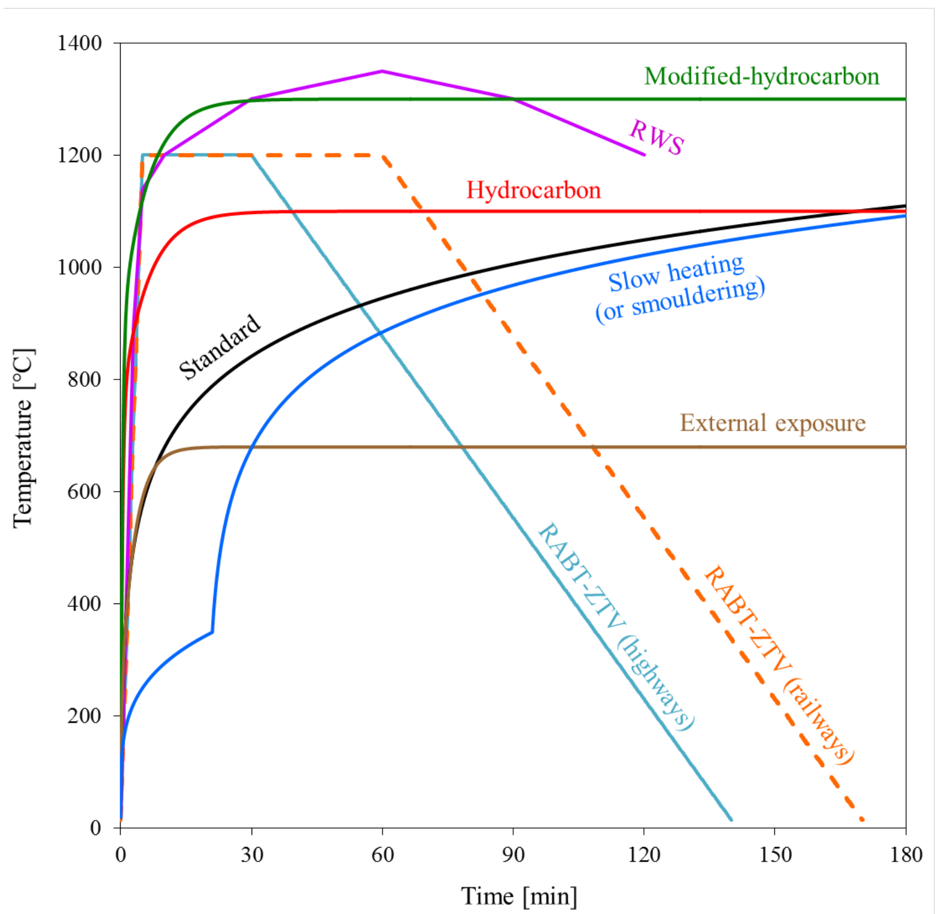

Figure 1 – The wide range of prescribed time-temperature curves.

2 THE CONTROL VARIABLE IN FIRE RESISTANCE TESTING

The boundary conditions of a thermodynamic system (e.g. a compartment fire, standard furnace test) are governed by conservation of energy [28], and are therefore typically formulated in terms of heat fluxes. This section presents a comparison of thermal boundary conditions defined by controlling the time-history of 'a temperature' inside a furnace (or oven), versus one defined by controlling the time-history of incident radiant heat flux at a specimen's exposed surface. Despite controlling for the same time-temperature curve, furnace testing standards worldwide require the use of different types of temperature gauges to measure temperatures inside furnaces, including: bare thermocouples (in Europe prior to 1999 [51]), plate thermometers (currently in Europe [29]), or shielded thermocouples (currently in North America [40]). In the current paper, the authors denote the temperature inside a furnace as 'a temperature,' however this temperature is that being measured by the specific type of temperature gauge used.

2.1 Control by Temperature

The transient enthalpy inside a furnace can be expressed by equating the heat inputs and outputs in the thermodynamic system [52]. Herein, the heat input is defined by the heat of combustion at the burners in the furnace. The heat output is defined by the energy going into the solid boundaries of the system (i.e. furnace linings and specimen), along with the energy advected out of the furnace through hot gases leaving the furnace (extraction vents) and fresh (ambient) air coming into the furnace. For a thermodynamic system in which the time-history of temperature $\left(\frac{\partial T}{\partial t}\right)$ inside the control volume (i.e. inside the furnace) is the control variable (or objective function), conservation of energy can be expressed as:

$$\Delta\dot{Q} - \dot{q}''_{net,lining} \cdot A_{lining} - \dot{q}''_{net,s} \cdot A_s = V_g \rho_g C_{p,g} \frac{\partial T}{\partial t} \tag{4}$$

Where the thermal equilibrium is defined by:

- the differential between heat inflow and outflow in the furnace ($\Delta\dot{Q}$);
- the net heat flux ($\dot{q}''_{net,lining}$) and exposed surface area (A_{lining}) of the furnace lining;
- the net heat flux ($\dot{q}''_{net,s}$) and exposed surface area (A_s) of the test specimen; and
- the enthalpy associated with gases inside the furnace ($V_g \rho_g C_{p,g} \frac{\partial T}{\partial t}$).

The volume inside the furnace is denoted as V_g. The density and specific heat of the gases inside the furnace are denoted by ρ_g and $C_{p,g}$, respectively.

$\Delta\dot{Q}$ is thus defined as:

$$\Delta\dot{Q} = \dot{m}_F \, \Delta H_{c.F} \; - \; \dot{m}_g \, C_{p,g} \, (T - T_{IN}) \tag{5}$$

Where the first term is the increased enthalpy due to the combustion process at the burners in the furnace, defined by the mass flow of fuel consumed by the burners ($\dot{m}_F$) and the heat of combustion of the fuel ($\Delta H_{c,F}$). The second term is defined as the differential enthalpy between the gases leaving the furnace at temperature T, and the gases coming into the furnace at temperature T_{IN}; where $\dot{m}_g$ and $C_{p,g}$ are the mass flow and specific heat of the gases leaving and entering the furnace, respectively.

The actual magnitude of the terms in Equation 5 is not relevant to the current discussion. To maintain $\frac{\partial T}{\partial t}$ by controlling a time-history of temperature inside the furnace, the furnace operates by controlling $\dot{m}_F$ (and $\dot{m}_g$ to some extent) so that $\Delta\dot{Q}$ compensates for the changes in the thermodynamic system; for example, changes in the thermal properties of the test specimen. Therefore, the magnitude of the terms that define $\Delta\dot{Q}$ cannot be generalized.

In practice, heating the inside of a furnace (or oven) is usually accomplished by forcing hot gases into the furnace using gas-fired burners (or less commonly using electrical heating coils). A representation of Equation 4 is given in Figure 2.

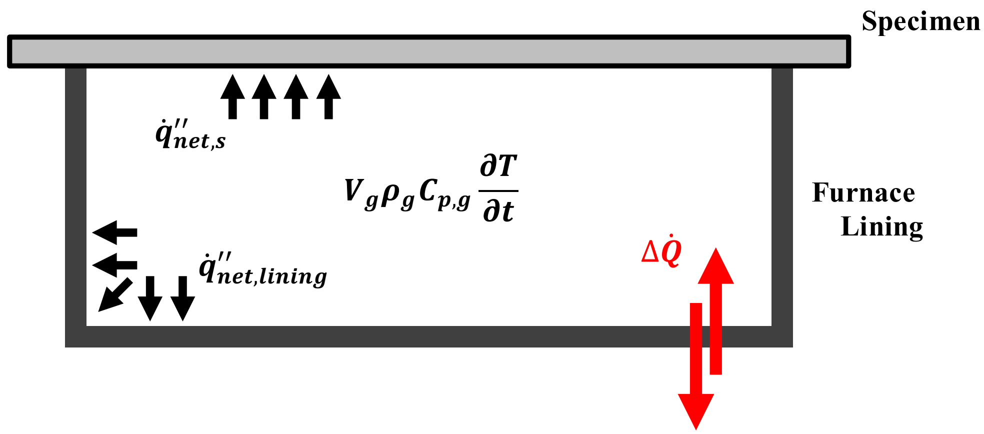

Figure 2 – Simplified energy conservation schematic of thermal boundary conditions for which the time-history of temperature is the objective function.

Equations 4 and 5 assume:

- homogenous temperature inside the furnace (i.e. within the control volume);
- homogenous net heat fluxes at the exposed surfaces of the furnace linings and the specimen;
- heat losses from hot gas extraction vents inside the furnace are neglected; and
- the kinetic and potential energy associated with the transient mass transfer of the gases inside the control volume are neglected.

The thermal boundary conditions at the exposed surfaces of a test specimen thus depend on the thermal state at the exposed surfaces, hence on the thermal properties (i.e. thermal inertia) of the materials being tested. Thus, while furnace lining materials, dimensions, temperature gauges, and specific burner types are now reasonably standardized and regulated (e.g. [29]), the thermal boundary conditions at the exposed surfaces of test specimens are inevitably linked to the thermal properties of the test specimen itself; making the comparative usefulness of tests controlled in this manner questionable for materials with different thermal properties [53]. Likewise, adoption of the *plate thermometer* as the standard gauge for temperature control within testing furnaces [29, 46] is also governed by energy conservation inside a furnace; hence precluding the notion that using a specific type of temperature gauge can fully harmonize the thermal boundary conditions imposed when controlling by a temperature [54, 55].

The variability of thermal properties for typical building and furnace lining materials (refer to Table 1) and its influence on the thermal boundary conditions at the exposed surfaces of a test specimen has motivated various research studies (e.g. [52, 56, 57, 58, 59]). These have all arrived to the conclusion that when the time-history of a temperature inside a furnace is the control variable, the thermal boundary conditions at the exposed surface are considerably and inevitably dependent on the furnace linings, emissivity of the gases, and thermal properties the test specimen itself. Current testing standards limit furnace lining materials to a maximum density, minimum thickness, and minimum exposed surface inside the furnace (e.g. [29]). Nonetheless, the divergence in thermal properties of normal building construction materials can be large (refer to Table 1), and this reduces the chances of true standardisation of the thermal boundary conditions using this approach.

Within the structural fire testing community, it is generally accepted that controlling the time-history of temperature inside a furnace is equivalent to controlling the thermal boundary conditions (or thermal exposure) at the exposed surface of the test specimen. Notwithstanding improvements that have been realised through the introduction of plate thermometers for controlling fire testing furnaces (in many jurisdictions), this still partly neglects the complex thermal interactions between the gases, linings, and specimen [11, 53, 60, 61]. The research presented in the current paper aims to address some of these shortcomings and to develop a complimentary fire testing method that directly controls incident radiant heat flux at the exposed surface of a test specimen.

Table 1 – Thermal properties of typical building construction materials and furnace lining materials.

		Density [kg/m^3]	**Thermal Conductivity** [W/mK]	**Specific Heat** [J/kgK]	**Thermal Diffusivity** [$m^2/s \times 10^{-9}$]	**Thermal Inertia** [$W s^2/K^2 m^4$]
Typical Building Construction Materials [62]	Aluminium	2,400	237	900	109,722	511,920,000
	Steel	7,800	40	466	11,005	145,392,000
	Concrete	2,000	2.5	880	1,420	4,400,000
	Plasterboard	800	0.17	1,100	193	149,600
	Expanded Polystyrene	20	0.003	1,300	115	78
Furnace Lining Materials [63]	BAM[1]	1,000	0.45	995	452	447,750
	CSTB[2]	1,250	0.55	1,080	407	742,500
	CSE[3]	2,000	1.10	1,500	367	3,300,000
	LPC[4]	880	0.33	1,110	338	322,344

[1] BAM: Bundesanstalt für Materialforschung und –prüfung, Germany
[2] CSTB: Centre Scientifique et Technique du Bâtiment, France
[3] CSE: Centro Studi ed Esperienze, Italy
[4] LPC: Loss Prevention Council, UK

If heat from the thermodynamic system going into the test specimen can be neglected (refer to Equation 4), the energy conservation in the furnace becomes independent of the test specimen. In a furnace this might be reasonable for materials with very small exposed surface areas (relative to the exposed surfaces of the furnace lining) and similar thermal properties to those of the furnace linings; otherwise this assumption is not valid. The following section describes a thermodynamic system where incident radiant heat flux is directly controlled, and energy conservation is therefore independent of the thermal properties of the sample being tested.

2.2 Control by Incident Radiant Heat Flux

For a system in which the control variable is the time-history of incident radiant heat flux ($\dot{q}''_{inc}$) at the exposed surface of the test specimen, the local energy conservation equation can be expressed as:

$$\dot{q}''_{net,s} = \alpha_s \, \dot{q}''_{inc} - \dot{q}''_{losses} \tag{6}$$

Where the net heat flux ($\dot{q}''_{net,s}$) is calculated accounting for the absorptivity (α_s) and heat flux losses ($\dot{q}''_{losses}$) at the exposed surface of the test specimen (refer to Figure 3). Hence the time-history of incident radiant heat flux ($\dot{q}''_{inc}$) is an independent control variable. The heat flux losses at the specimen's exposed surface may be calculated using a direct heat transfer model (analytical or numerical, implicit or explicit). For instance, a simplified formulation for calculating the heat flux losses at the exposed surface is:

$$\dot{q}''_{losses} = h_c(T_s - T_{amb}) + \varepsilon_s \, \sigma \, T_s^4 \tag{7}$$

where constant or temperature dependent values may be considered for the convective heat transfer coefficient (h_c) and emissivity (ε_s) (e.g. [8], [30]).

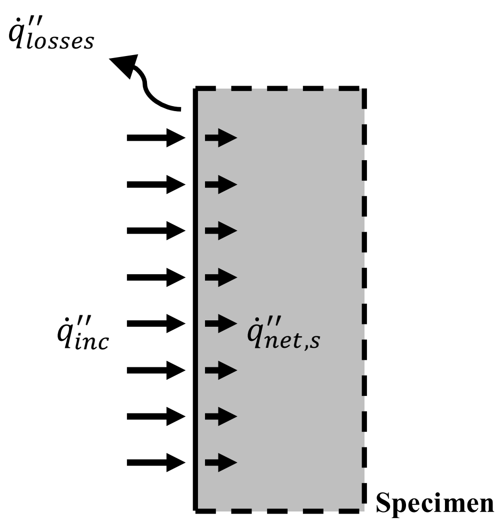

Figure 3 – Simplified energy conservation schematic of a thermal exposure for which the time-history of incident radiant heat flux is the objective function.

Control of fire science experiments by incident radiant heat flux is not a novel concept [56]; indeed it has been widely implemented for more than five decades in a wide variety of fire science studies (e.g. [64, 65, 66, 67, 68, 69, 70]). Commercially available fire testing apparatus such as the *Cone Calorimeter* [71, 72] or *Fire Propagation Apparatus* [73, 74] are widely used for small-scale tests with control by incident radiant heat flux. Furthermore, numerous authors have suggested replacing a prescribed time-history of temperature when describing a fire with a time-history of incident radiant heat flux (e.g. [11, 14, 54, 56, 61, 75, 76, 77, 78]). This is the approach taken in the current research.

3 THE HEAT-TRANSFER RATE INDUCING SYSTEM (H-TRIS) TEST METHOD AND APPARATUS

To address issues associated with performing fire testing by controlling a temperature rather than heat flux, a novel test method and apparatus was developed. The Heat-Transfer Rate Inducing System (H-TRIS) allows for direct and independent control of the thermal boundary conditions imposed on a test specimen by controlling a specified time-history of incident radiant heat flux at its exposed surface [79].

The first generation apparatus, H-TRIS Mark 1, uses a mobile array of propane-fired radiant panels, along with a mechanical linear motion system and a rotary stepper motor (see figures 4 and 5). The linear motion system can be programed to actively control the relative position between the radiant panels and the exposed surface of a test specimen.

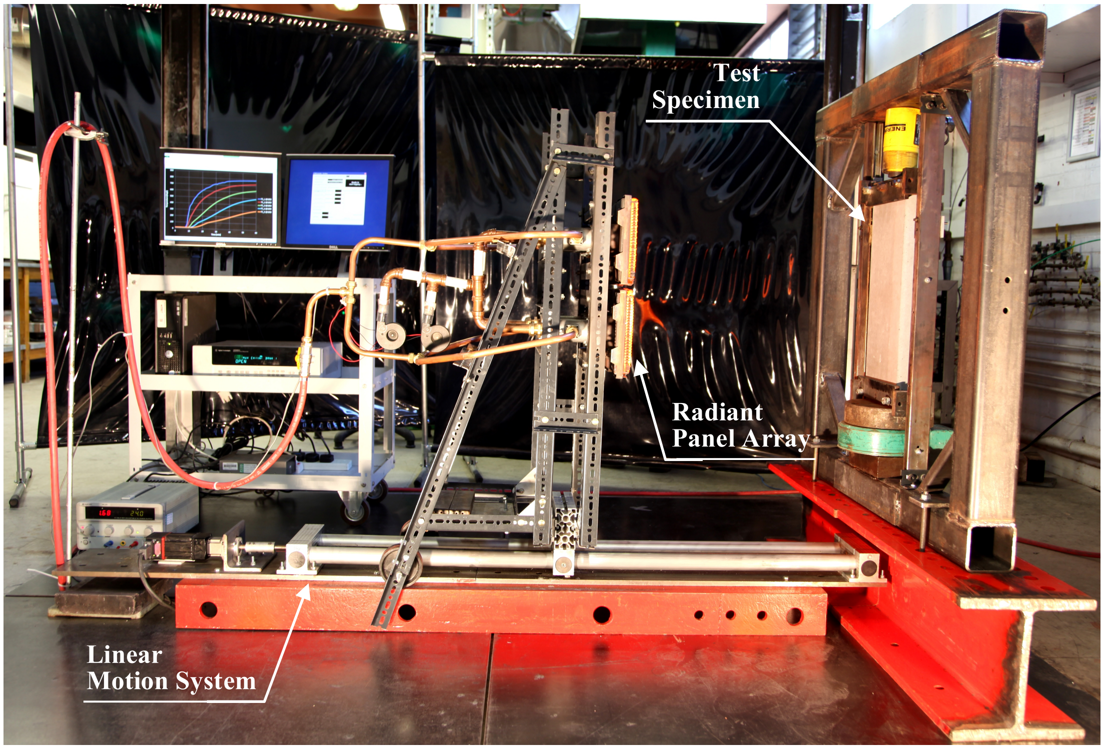

Figure 4 – Photograph of H-TRIS Mark 1 (side elevation).

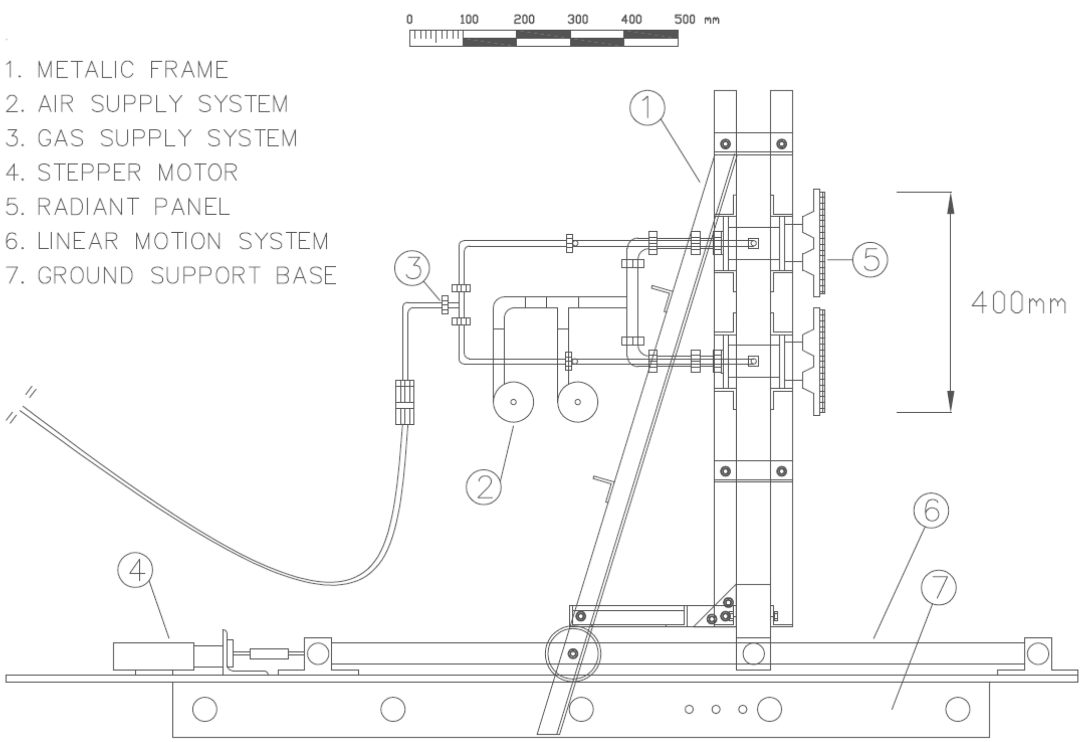

Figure 5 – Schematic of H-TRIS Mark 1 (side elevation).

3.1 Control of the Thermal Boundary Condition

The radiant panel array is pre-set to operate at a constant panel temperature, thus the heat output (Q_{panels}) is monitored by controlling the mass flow of air and propane to the panels, assuring a steady operation. The incident radiant heat flux at the target surface of the test specimen (q''_{inc}) is measured during a pre-test calibration procedure, by positioning a Schmidt-Boelter heat flux gauge [80] at an offset distance, x, from the radiant panel array (see Figure 6).

The time-history of net heat flux at the exposed surface of the test specimen may be defined as shown in Equation 6 and schematically represented in Figure 7. For example, if the objective is to replicate a required net heat flux ($\dot{q}''_{net,s}$), an inverse heat transfer model may be used to calculate the incident radiant heat flux which yields the desired net heat flux, while also accounting for the thermal boundary conditions (absorptivity and heat losses) at the exposed surface of the test specimen (refer to Section 4).

H-TRIS is operated to ensure sufficient spatial separation between the radiant panels and the exposed surface of the test specimen to avoid imposition of vitiated air near the surface of a specimen, thus supporting the assumption used in the inverse modelling procedures that heat gain is by radiation, and gases at the exposed surface of the test specimen are not directly influenced by convective currents from the radiant panels themselves [65].

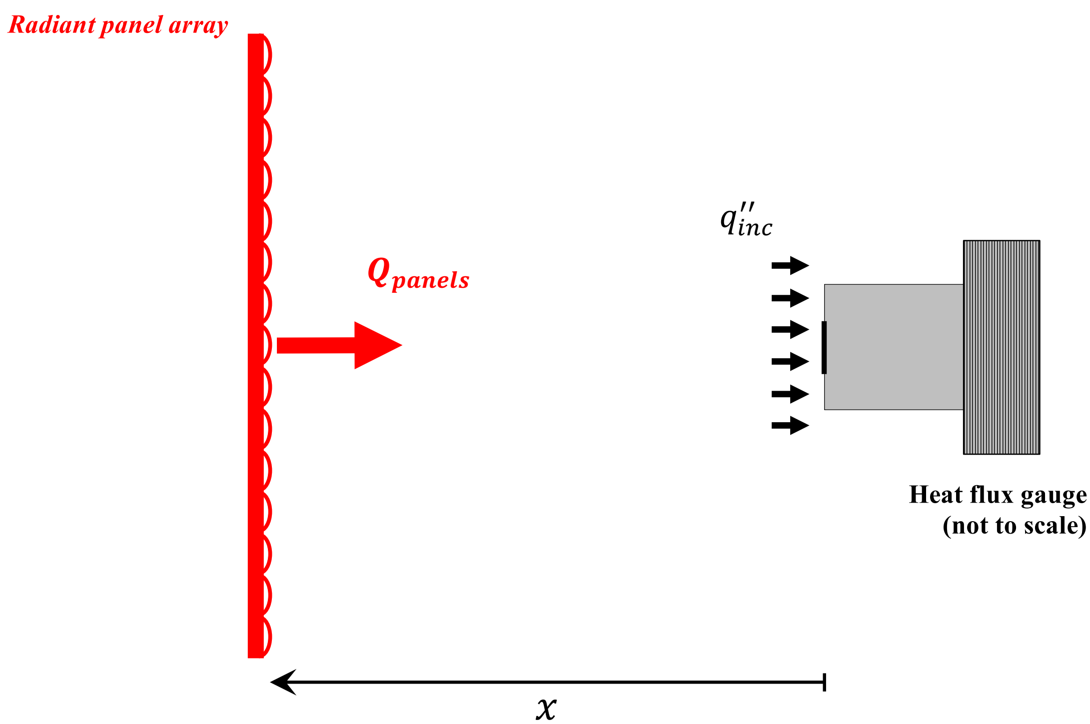

Figure 6 – Simplified schematic of H-TRIS during pre-test calibration, and energy conservation at the exposed surface of the Schmidt-Boelter heat flux gauge used in calibration.

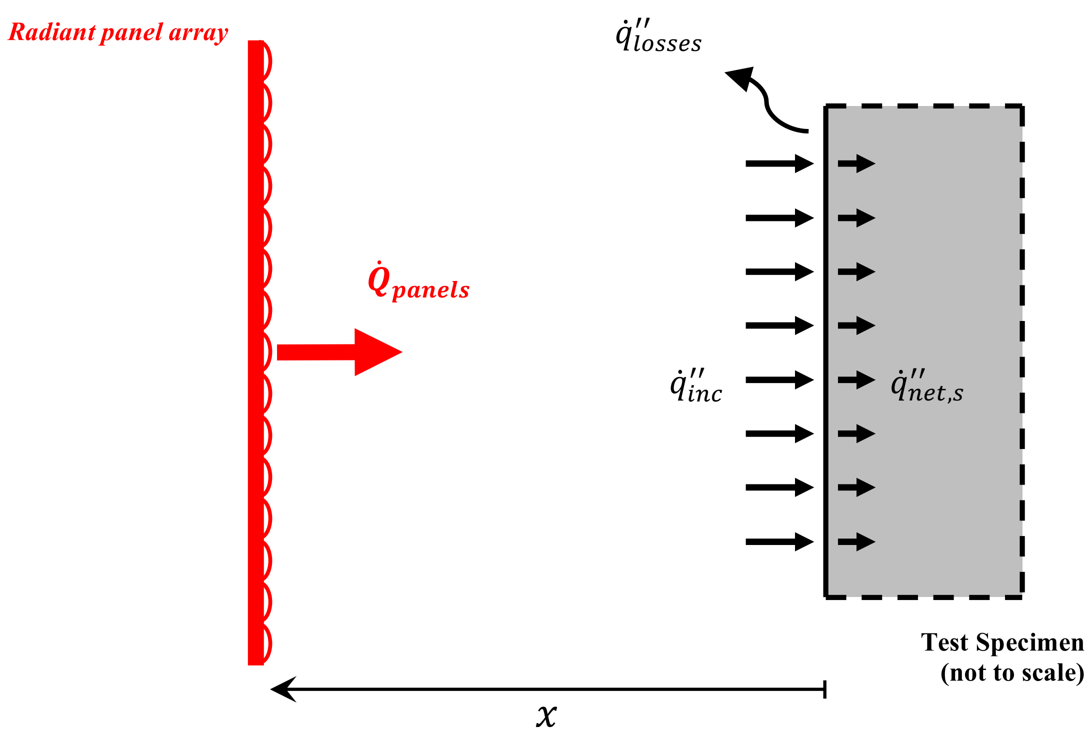

Figure 7 – Simplified schematic of H-TRIS during testing and energy conservation at the exposed surface of the test specimen.

Using this approach, H-TRIS is able impose a controlled net heat flux, and thus the in-depth time dependent temperature distribution in solid media can be directly controlled during testing. This is a non-trivial advantage for the fire safe characterization of building construction materials, since unlike traditional fire testing furnaces, it allows explicit control and quantification of the heating rates within thermally thick materials (e.g. concrete, timber, polymer foams, etc.). Figure 8 shows the time-history of incident radiant heat flux imposed with H-TRIS during a study of heat induced concrete spalling. These boundary conditions aimed at yielding an equivalent time-history of net heat flux to that experienced by specific concrete test specimens during a fire resistance test in a furnace. The details of this study are presented in Section 4.

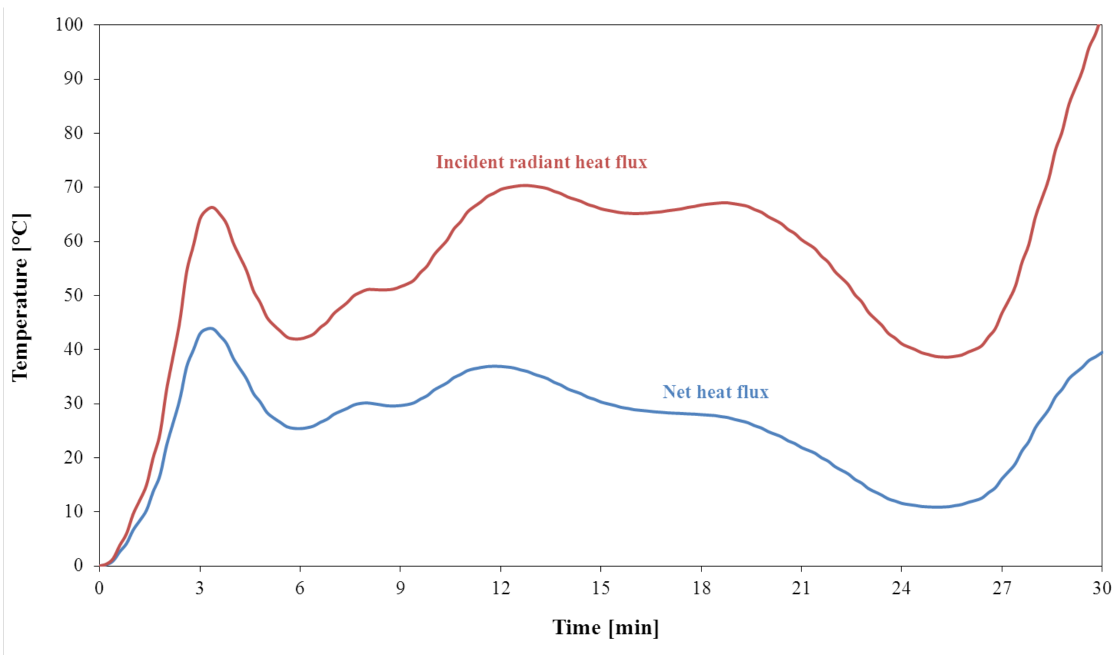

Figure 8 – Time-history of net heat flux during a standard fire resistance test and calibrated incident radiant heat flux imposed using H-TRIS, yielding an equivalent net heat flux at the exposed surface of a concrete test specimen.

3.2 Technical Aspects

This paper presents the heat transfer theory behind the H-TRIS testing methodology, while also providing a detailed description of the technical aspects of the H-TRIS Mark 1 test apparatus (see figures 4 and 5). In collaboration with the authors, other testing laboratories (e.g. The University of Queensland, Australia and the Technical University of Denmark, DTU) are currently developing similar H-TRIS apparatus. These, while following the same fundamental approach, are intended to allow for multiple and/or larger exposed surfaces and higher heat fluxes.

3.2.1 Radiant Panel Array

Four high-performance propane-fired radiant panels are mounted to a metal frame to form a 200 × 400 mm^2 array of radiant panels (Figure 9). The commercially available radiant panels operate using a combustion process that takes place within a 3.5 mm (± 0.2 mm) thick sintered metal fibre medium. This results in a lightweight radiant panel with rapid thermal response (during both heating and cooling), high and stable operational temperature, and thermal homogeneity at the emitting surface.

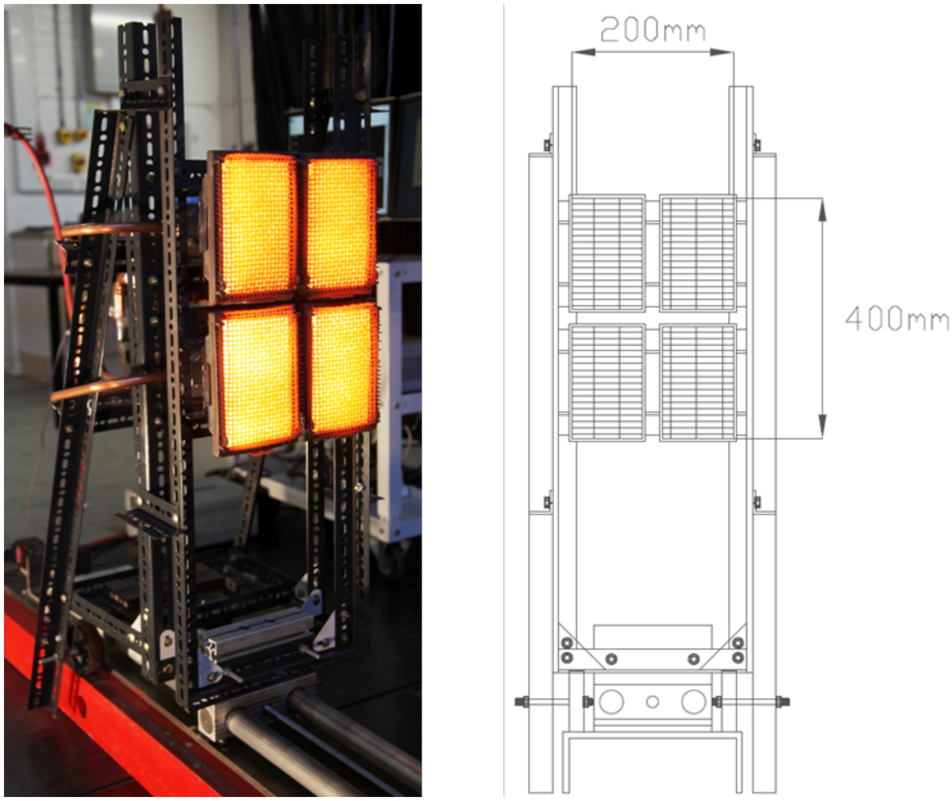

Figure 9 – Photo and schematic showing propane-fired radiant panels for H-TRIS Mark 1 (front elevation).

3.2.2 Heat Flux Gauge

Incident radiant heat flux measurements at the target surface of test specimens are calibrated using a Schmidt-Boelter heat flux gauge (see Figure 10). It is known that hot gases accumulated around heat flux gauges significantly influence their incident irradiation measurements [81, 82], and that this may result in an underestimation of up to 20% when the gauge is placed flush with a target surface; this is due to free convective flows that are created by heating of the surface. Given that water-cooled heat flux gauges are calibrated under natural convection conditions, or alternatively in a vacuum [83], to minimise the influence of hot gases around the gauge, it is recommended that this type of heat flux gauge should not be mounted flush to a surface [81]. When calibrating H-TRIS the heat flux gauge was mounted on a self-cooling probe (Figure 10).

Figure 10 – Schmidt-Boelter heat flux gauge mounted on a self-cooling probe system designed to minimise the influence of convective flows near the gauge.

3.2.3 Linear Motion System

A mechanical linear motion system is used to hold the radiant panel array and supporting frame, and to control the array's relative position with the target surface, $x(t)$. A threaded rod is fixed to a computer-controlled stepper-motor, and aligned within the metallic frame holding the radiant panel array. This system was designed to automatically control the position of the radiant array with high speed and accuracy.

3.3 Testing Operation of H-TRIS

3.3.1 Pre-test Calibration Procedure

Pre-test calibrations are performed periodically to obtain the correlation between relative position of the radiant panels and the incident radiant heat flux at the target surface, $x(q''_{inc})$. Calibrations can be repeated to account for specific changes in setup or conditions on any given day (e.g. panel performance and wear), thus ensuring repeatability between tests.

During calibration the heat flux gauge is placed at the intended target surface location, and the relative position of the radiant panel array is automatically varied from the maximum to the minimum distance to the heat flux gauge. Incident radiant heat flux readings obtained in this manner are then used to generate a curve of incident radiant heat flux versus distance from the radiant panels (for example Figure 11). The heat flux gauge is placed at the centre of the target surface. In its current incarnation, H-TRIS Mark 1 has a range yielding minimum and maximum incident radiant heat fluxes of 5 and 130 kW/m^2, respectively (see Figure 11).

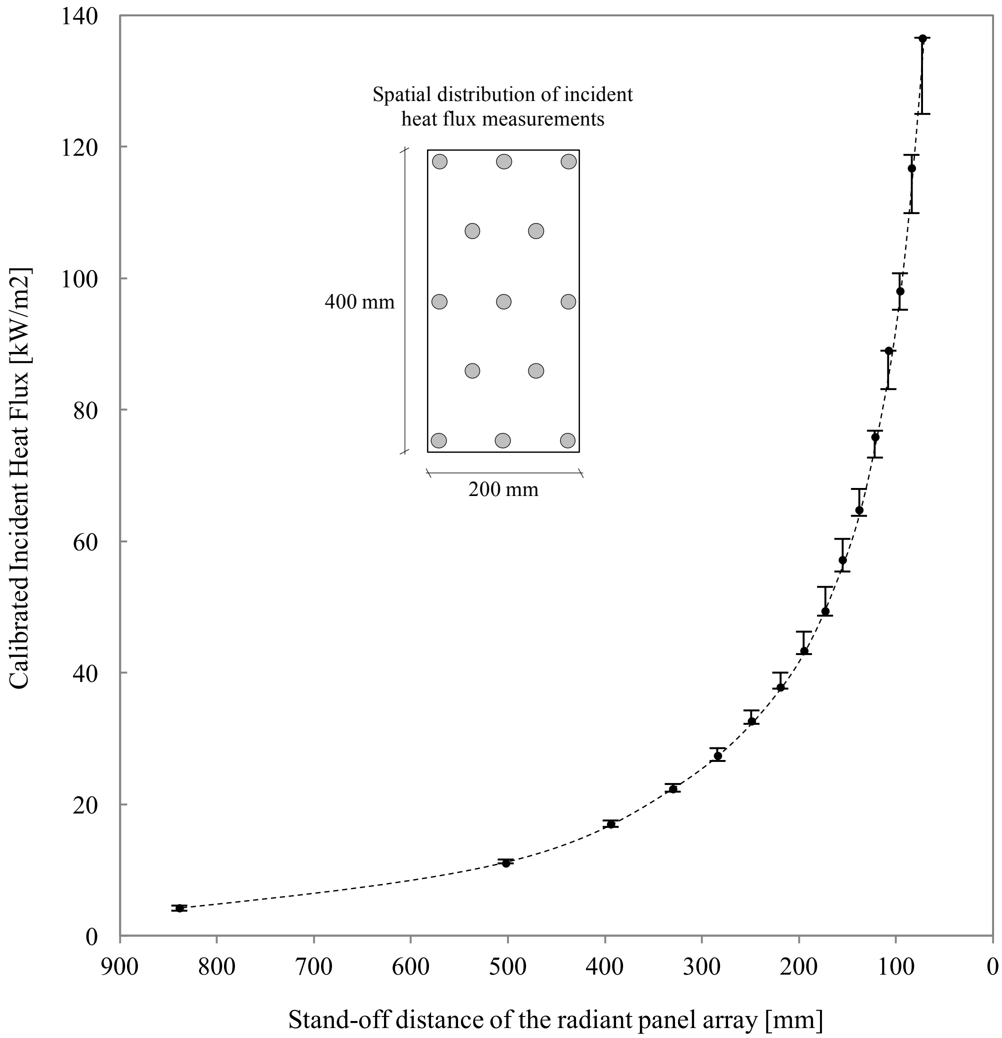

Figure 11 – Typical calibration results for incident radiant heat flux at the centre of the target surface versus stand-off distance of the radiant panel array. Error bars show range of deviation for spatial distribution of measured incident radiant heat flux relative to measurements taken at the centre of the target surface.

3.3.2 Testing Procedure

The time-history of the stand-off distance of the radiant panel array (i.e. relative distance between the array and the target surface) is expressed as $x(t)$, and is calculated by inputting the desired time-history of incident radiant heat flux function, $q''_{inc}(t)$ into the pre-test calibration function, $x = f(q''_{inc})$. Hence, the formulation of the time-history of relative position of the radiant panels is calculated as:

$$x(t) \; = \; f\left(q''_{inc}(t)\right) \tag{8}$$

The above can either be described as a continuous function or as discrete values. Using this approach, a wide range of time-histories of incident radiant heat flux can be recreated. This makes H-TRIS considerably more versatile than a fire testing furnace, and is limited only by the range of incident radiant heat fluxes achieved during the calibration process. In turn, this is defined by the size and type of radiant panels used, the minimum and maximum distances between radiant array and the target surface, and the speed of the linear motion system.

3.3.3 Spatial Distribution of Thermal Boundary Conditions

An assessment of the spatial distribution of incident radiant heat flux at the target surface is periodically measured to ensure uniformity of the imposed heat flux. This procedure is performed in the same manner as that described for the pre-test calibration; however, the procedure is repeated for various locations on the target surface (refer to Figure 11). For example, for the study presented in this paper, it was intended for concrete specimens having an exposed surface area of 200 × 400 mm^2. Thus, the spatial distribution of incident radiant heat flux was assessed at the locations shown in Figure 11. The spatial distribution of incident radiant heat flux was better than 90% uniform. The spatial distribution of heat flux at the target surface is will obviously depend on the ratio between the area of the target surface and that of the radiant panel array.

4 APPLICATION TO STUDIES ON HEAT-INDUCED CONCRETE SPALLING

A number of research-driven and product development projects have already been undertaken using the H-TRIS test method for studying fire-related aspects for a range of building construction materials and system assemblies (e.g. highly optimized prestressed concrete slabs [84], lightweight structural concrete sandwich elements [85], concrete tunnel lining segment materials [86], intumescent coatings [87], cross laminated timber [88], non-metallic dowelled timber connections [89], and building insulation materials [90]). This section illustrates application of H-TRIS within a project studying heat-induced concrete spalling.

A thorough review of past experimental work studying heat-induced concrete spalling [79] is avoided here, but highlighted the wide range of factors that have previously been suggested as influencing the propensity for concrete spalling in fire. Maluk [79] has shown that the many prior studies on concrete spalling have yielded somewhat contradictory results. For instance, some studies have shown that higher heating rates result in greater propensity for spalling (e.g. [91]), however in some cases slower heating has actually shown more severe spalling (e.g. [92]).

Heat-induced explosive concrete spalling occurs when the exposed surface of concrete is heated, and it flakes away in a more or less violent manner [84]. As a consequence, the concrete cover to the internal reinforcement may be reduced, possibly resulting in rapid temperature increases in the internal reinforcement and within the core of the structural element in addition to a direct influence on load bearing capacity due to the loss of physical or effective cross sectional area. Heat-induced concrete spalling presents a potentially serious concern in the context of the historical approach to fire safe structural design of concrete structures, and the fire resistance community continues to investigate the causes and implications of the apparent increased propensity for spalling of modern concrete mixes [79], particularly those with high strength and/or self-consolidating properties.

Numerous experimental studies have shown that inclusion of polypropylene (PP) fibres in fresh concrete can reduce concrete's propensity for heat-induced spalling [79]. Polypropylene fibres are theorised to alter the transient moisture migration and/or evaporation processes within heated concrete, thus mitigating spalling (particularly when a thermo-hydraulic – i.e. pore pressure – spalling mechanism is dominant). The relative importance of the physical mechanisms that may explain the effectiveness of PP fibres in reducing concretes' propensity for heat-induced concrete spalling remains a matter of debate [93]. Regardless of this debate, current design and construction guidance for mitigation of spalling is based on adding a typical dose of PP fibres (i.e. mass of PP fibres per volume of concrete) for concrete mixes or end use conditions in which spalling is considered likely to occur [94]. Physical mechanisms aside, it is reasonable to assume that an optimum (or most 'effective') PP fibre type and dose will exist to mitigate spalling under a given set of mechanical and thermal conditions [95]. Since it is not currently possible to model the occurrence of spalling, and due to the complexity of and uncertainty of the various mechanisms possibly contributing to spalling and the potential mechanisms behind PP fibres' effectiveness, an experimental study on the effectiveness of PP type and dose was performed using the H-TRIS testing method and apparatus.

4.1 Aims of the Study on Spalling

H-TRIS was used to test a large number of medium-scale concrete specimens during severe heating. This was accomplished at a low economic and temporal cost, and with outstanding repeatability as compared with testing multiple samples in a traditional fire testing furnace. The propensity for heat-induced spalling was examined for eleven high-performance, self-consolidating concrete (HPSCC) mixes for which PP fibre type, cross-section, length, supplier, and dose were systematically varied. Rather than seeking to unravel and understand the precise mechanisms contributing to spalling or defining the fire resistance (in the time domain) of structural elements incorporating these specific concrete mixes, the study described herein aimed to evaluate the propensity for spalling of the concrete mixes tested under repeatable heating exposures and mechanical conditions; simulating the thermal conditions experienced by concrete specimens during a standard furnace test. Since the concrete mixes evaluated within this study were developed to be used in slender, highly optimized concrete elements, there was a need to completely avoid spalling. Heating of the specimens was therefore terminated as soon as the first significant spalling event occurred.

4.2 Spalling Tests using H-TRIS

The thermal exposure imposed with H-TRIS for the spalling study aimed to replicate that experienced by concrete specimens measured during large-scale fire resistance tests of similar specimens and concrete mixes [96]. These were the first experiments ever performed using H-TRIS to *simulate* the net heat flux at the exposed surface, and hence the in-depth time dependent temperature distributions within concrete specimens, during a standard fire resistance test. The time-history of incident radiant heat flux imposed with H-TRIS yielding an equivalent time-history of net heat flux (see Figure 8) to that experienced by concrete test specimens during a fire resistance test, was calculated using an inverse heat conduction model developed by the authors [79]. Is noteworthy that, unlike a traditional direct heat conduction model in which the thermal boundary conditions are assumed and used as an input to calculate the in-depth time dependent temperature distribution within a solid, an inverse heat conduction model uses measured in-depth time dependent temperature distributions as inputs to calculate the thermal boundary conditions. A thorough description of the inverse heat conduction model is presented elsewhere [79].

Due to the maximum proximity of the radiant panel array with respect to the exposed surface of the specimens in the spalling study (refer to Figure 4), the maximum possible incident radiant heat flux was 100 kW/m^2. Thus, the desired time-history of incident radiant heat flux (shown in Figure 8) was imposed until an incident radiant heat flux of 100 kW/m^2 was reached; beyond this point the incident radiant heat flux was maintained constant at 100 kW/m^2. If no spalling occurred within 60 minutes of heating the test was halted, since heat-induced explosive spalling is unlikely to occur at such a late stage [84].

Figure 12 shows a comparison of in-depth temperature measurements recorded for concrete specimens during a large-scale standard fire resistance test on otherwise identical specimens in the thermal domain [96] against those measured at the same locations during tests using H-TRIS (with H-TRIS programmed on the basis of the inverse model described in [77] to simulate the furnace exposure). Test specimens were considered to be identical in the thermal domain, given that the boundary conditions and parameters that control the heat conduction processes were effectively identical (cross-section of the test specimens and thermal properties of the concrete). The shaded areas in Figure 12 represent the spread of in-depth temperature measurements in five large-scale concrete test specimens tested simultaneously during a single standard furnace test, whereas the black lines represent the equivalent measurements taken during a series of individual tests on effectively identical (in the thermal domain) specimens tested with H-TRIS (three individual thermocouple readings are shown for each specimen at 10, 20 and 45 mm from the exposed surface). The solid lines terminate at the instant that the individual tests in H-TRIS were stopped. Figure 12 shows that the H-TRIS methodology is able to accurately replicate the in-depth time dependent temperature distribution experienced by concrete specimens during a standard fire resistance test. H-TRIS also appears to be more accurate and repeatable, both within individual tests and across multiple repeat tests. The temperature deviation of the measurements taken from the eight plate thermometers inside the standard furnace was compliant with the testing standard [29].

Given that the end use application for the specific HPSCC mixes examined in this study involves highly optimized prestressed concrete systems [96], there was a need to examine the effect of pre-compressive stresses acting on the concrete during testing. Mechanical loading and boundary conditions were imposed using a purpose built loading rig, designed to impose a sustained axial compressive load to the test specimens during heating [79]; hence reproducing the pre-compression experienced by the specimens in service.

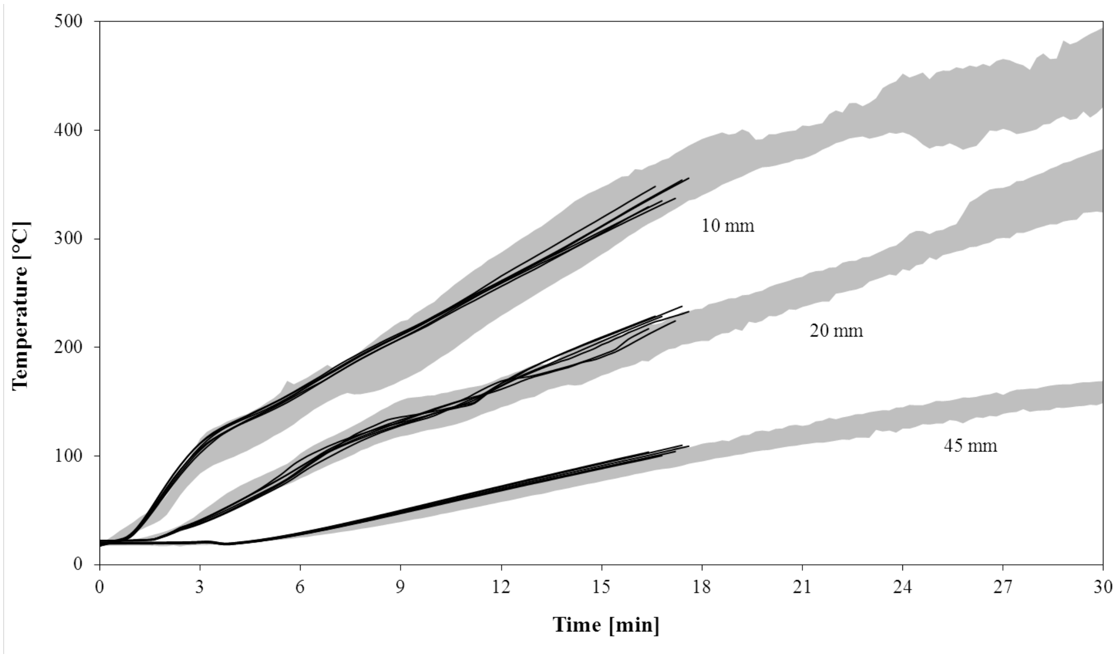

Figure 12 – In-depth temperature measurements taken during a standard fire resistance test [96] compared against those made with H-TRIS (shaded areas show the spread of the measurements during the furnace test, black lines show measurements with H-TRIS).

4.3 Spalling Test Programme

Constrained by requirements on minimum strength and self-compaction of the concrete mixes, the concrete compressive strength (C90 according to [94]) and workability (slump flow of 750 mm according to [97]) were maintained constant for all concrete mixes examined in the spalling study. Parameters assessed amongst the concrete mixes were:

- PP fibre cross-section (18 or 32 μm diameter circular cross-sections, and 37 × 200 μm^2 rectangular cross-sections);
- PP fibre length (3, 6, 12, or 20 mm);
- PP fibre type (monofilament, multifilament, or fibrillated);
- PP fibre supplier (three manufacturers: Bekaert, Propex, and Vulkan); and
- PP fibre dose (between 0.68 and 2.34 kg per m^3 of concrete).

While only the abovementioned concrete mix parameters were intentionally varied, other mild variations were required during concrete mixing so as to attain the minimum required slump flow of 750 mm. This was mainly attributed to inclusion of various types and amounts of PP fibres; however these variations are not considered relevant within the context of the current work [79].

Medium-scale unreinforced and unstressed concrete specimens were tested using H-TRIS in a vertical orientation with heating from one side. Recognising that scaling of test specimens in structural fire resistance testing is debated on various grounds [79], the dimensions in the direction of the principal heat flow were taken as the same as used in prior standard furnace tests of large-scale specimens [96]. Thus, medium-scale specimens were cast with identical cross-sections as the large-scale fire resistance test specimens: 45 × 200 mm^2. The length of the H-TRIS specimens was limited to 500 mm due to space limitations, with cold overhangs (i.e. unheated ends) of 50 mm in length; the thermally exposed surface was 400 × 200 mm^2.

Specimens were tested either under a free-to-expand (unrestrained) condition or under sustained compressive load to give a concentric axial compressive stress of 12.3 MPa [79]. Load was applied using notionally rotationally fixed-fixed end conditions, and held constant for the duration of the tests using a hydraulic load control system (i.e. the applied compressive load was maintained constant, partly counteracting potential effects from thermal expansion and elastic modulus changes of the test specimen during heating). Unloaded test specimens were left free-to-expand (under notionally rotationally pinned-pinned end conditions) during heating. All tests were performed in triplicate.

4.4 Results and Discussion

Sixty-six precisely controlled and repeatable spalling tests were performed during a period of 30 days; thus demonstrating the low temporal cost of the H-TRIS approach. It is noteworthy that contrary to expectations based on prior heat-induced concrete spalling experimental studies [79], when spalling occurred for a given mix it occurred for all three identical repeat tests and at similar heating exposure times. Likewise, if no spalling was observed for a particular mix then this was true for all three repeat tests. During testing, spalling occurred for four of the 11 concrete mixes assessed. Spalling occurred for concrete mixes including:

- no fibres;
- PP fibres of 32 μm diameter circular cross-section, 3 mm long, multifilament, at a dose of 1.20 kg per m^3 of concrete;
- PP fibres of 37 × 200 μm^2 rectangular cross-sections, 20 mm long, fibrillated, at a dose of 1.20 kg per m^3 of concrete; and
- PP fibres of 37 × 200 μm^2 rectangular cross-sections, 20 mm long, fibrillated, at a dose of 2.00 kg per m^3 of concrete.

None of the other mixes experienced any spalling whatsoever for the full duration of the 60 minutes test. Figure 13 shows typical post-test photographs of three specimens demonstrating increasing severities of spalling (i.e., surface spalling, mild spalling, and destructive spalling).

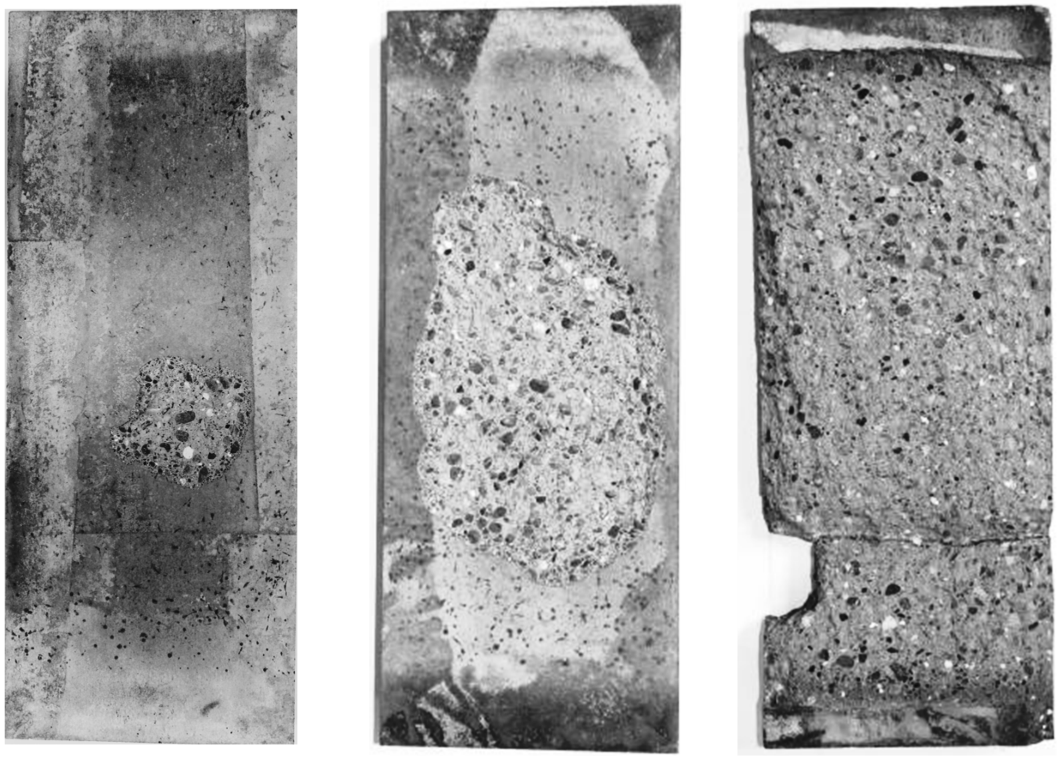

(a) Surface spalling *(b) Mild spalling* *(c) Destructive*

Figure 13 – Typical specimens after tests using H-TRIS, demonstrating (a) surface, (b) mild, and (c) destructive spalling.

A complete description and analysis of the results from this experimental study are presented elsewhere [79, 84]. The following observations were made based on the parameters varied between specimen sets:

- *PP fibre cross section* – Inclusion of PP fibres with smaller cross sections appeared to have a positive influence in mitigating spalling for both loaded and free-to-expand specimens.
- *Fibre length* – Concrete mixes cast with relatively short (3 mm long) monofilament PP fibres exhibited a higher risk of spalling than practically identical mixes (equivalent PP fibre doses) with longer fibres (6 or 12 mm long). Thus, longer PP fibres (presumably up to some as yet unknown optimal length) appeared to be more effective at mitigating heat-induced spalling.

- *Fibre supplier* – The PP fibre supplier has no obvious influence on test results, all other factors being equal.

- *Fibre type* – Because the dimensions (cross section and length) of monofilament or multifilament, and fibrillated PP fibres assessed in this study diverged significantly, it is not possible to independently assess the influence of PP fibre type on the occurrence of spalling. Nonetheless, no obvious influence was observed for mixes cast with monofilament or multifilament PP fibres, all other factors being equal. Fibrillated PP fibres were less effective than monofilament PP fibres.

- *Fibre Dose* – As expected, high doses of PP fibres had a positive influence in mitigating the occurrence of spalling; however, some very low doses (0.68 kg of PP fibres per m^3 of concrete) of the smaller cross sections PP fibres (18 μm diameter) were also effective at mitigating spalling. The reasons for this are not yet clear.

- *Sustained Pre-Compressive Stress* – Tested specimens for which spalling occurred under sustained compressive load also suffered from spalling when tested under free-to-expand conditions. The exception to the above was for one of the mixes that included 2.00 kg of fibrillated PP fibres per m^3 of concrete; this mix spalled only when tested under sustained compressive load. Thus, a possible influence of pre-compressive stress was observed.

Using H-TRIS it was possible to accurately quantify the time-to-spalling and the mass spalled. Spalling consistently occurred between 7 and 25 minutes from the start of heating. The occurrence of heat-induced concrete spalling for specimens tested with H-TRIS was in reasonable agreement in terms of time-to-spalling (i.e. ±2 minutes) with specimens cast from identical concrete mixes and tested during prior standard furnace tests [84]. This result provides further evidence of H-TRIS' ability to accurately replicate not only the in-depth time dependent temperature distribution experienced by concrete specimens during a standard fire resistance test (see Figure 12), but also the time-to-spalling during repeat testing of effectively identical (from a thermal perspective) specimens under the same thermal boundary conditions.

4.5 Conclusions from the Study on Spalling

PP fibre dose is currently the primary parameter prescribed by design guidance (e.g. [94]) to mitigate spalling; however, the large number of experiments and repeatability of test results of this study reveals that fibre cross section and individual fibre length may also influence PP fibre effectiveness. These conclusions are strictly only valid for the heating conditions experienced by concrete specimens during tests with the specific standard furnace used to define the H-TRIS boundary conditions in the current study [96].

The current study represents the first attempt to use the H-TRIS testing method to replicate the thermal boundary conditions experienced by concrete specimens in a standard furnace test through medium-scale testing with mobile radiant panels. Additional research is needed to better understand the necessary mix design parameters to reliably prevent heat-induced concrete spalling under a range of service conditions and design fire exposures. However, the capability of H-TRIS to inexpensively, accurately and repeatable quantify the thermal conditions during a fire resistance test has been demonstrated.

5 CONCLUSIONS

This paper has presented a novel test method and apparatus, named H-TRIS (Heat-Transfer Rate Inducing System), that was first conceived for fire testing of construction materials and systems at medium-scale by directly controlling the thermal boundary conditions at an exposed target surface; this is accomplished by imposing a time-history of incident radiant heat flux. H-TRIS presents a complimentary test method to conventional material and structural fire testing in furnaces (or ovens), in which thermal boundary conditions are indirectly controlled by imposing a time-history of temperature.

H-TRIS is capable of imposing any desired time-history of incident radiant heat flux (within the bounds of the minimum and maximum flux that can be achieved), or of reproducing the in-depth time dependent temperature distributions within a solid for materials heated during a traditional fire test, large-scale fire test, real fire, or resulting from outputs from a fire model. Besides the scientific advantages associated with direct control of the thermal boundary conditions at the exposed surface of test specimens, other advantages of the method include:

- *The ability to impose a range of thermal exposures* – alongside the development of H-TRIS, an inverse heat conduction model was developed to calculate the time-history of incident radiant heat flux which yields an equivalent in-depth time dependent temperature distribution in a solid material during potentially any heating scenario.

- *Repeatability* – calibration runs are repeated periodically to account for specific changes in setup or environmental conditions, thus allowing a high level of repeatability between tests. Consequently, good statistical confidence for research studies carried out with multiple repeat tests, as is required for probabilistic assessment of materials that is needed in support of explicit structural fire safety design.

- *Operation at low economic and temporal costs* – experimental fire resistance research and development has historically been somewhat limited by the comparatively high economic and temporal costs associated with standard fire resistance testing in furnaces, thus a limited number of tests are typically performed for each test variable of interest. H-TRIS allows for multiple repeat tests to be performed at comparatively low cost, and to develop a stochastic understanding of material and element response to heating.

REFERENCES

[1] Law M. (1983). A Basis for the Design of Fire Protection of Building Structures. *The Structural Engineer*, 61 (1), 25-33.

[2] Plank R. (2013). Performance Based Fire Engineering in the UK. *International Journal of High-Rise Buildings*, 2 (1), 1-9.

[3] British Steel (1999). *The Behaviour of Multi-storey Steel Frame Buildings in Fire*. British Steel, Rotherham, UK, 82pp.

[4] Usmani A.F., Rotter J.M., Lamont S., Sanad A.M., and Gillie M. (2001). Fundamental Principles of Structural Behaviour Under Thermal Effects. *Fire Safety Journal*, 36 (8), 721-744.

[5] Lane B. and Lamont S. (2005). Arup Fire's Presentation Regarding Tall Buildings and the Events of 9/11. *Arup Fire*, London, UK.

[6] Torero J.L. (2011). Fire-induced Structural Failure: The World Trade Center, New York. *Forensic Engineering*, 164 (FE2), 69-77.

[7] Law M. (1981). Designing Fire Safety for Steel – Recent Work. *Proceedings of the ASCE Spring Convention, American Society of Civil Engineers*, New York, 16 pp.

[8] CEN (2004). Eurocode 2: Design of Concrete Structures – Parts 1-2: General Rules – Structural Fire Design (EN 1992-1-2:2004). *European Committee for Standardization*, Brussels, Belgium, 100 pp.

[9] Law M. (1995). The New Code of Practice (Part 1) – The Philosophy and Understanding. Presented at the *Seminar at AEA Technology,* Institution of Fire Engineers, Warrington, UK, 4-5 May, 4 pp.

[10] Grosshandler W. (2002). Fire Resistance Determination and Performance Prediction Research Needs Workshop: Proceedings (NISTIR 6890), *National Institute of Standards and Technology*, 124 pp.

[11] Torero J.L. (2013). Structures in Fire or Fires in Structures? Assessing the True Performance of Structures in Fire. *Proceedings of the 5th International Conference on Structural Engineering*, Cape Town, South Africa, 1919-1923.

[12] Buchanan A.H. (2001). *Structural Design for Fire Safety*. West Sussex, UK: John Wiley & Sons Ltd. 448 pp. ISBN: 9780471890607

[13] SFPE (2007). SFPE Engineering Guide to Performance-Based Fire Protection. *Society of Fire Protection Engineers*, USA, 207pp.

[14] Pettersson O. (1973). Need For and Some Remarks on Internationally Standardized Fire Test Procedures. *Lund Institute of Technology*, Lund, Sweden, 19 pp.

[15] SFPE (2004). SFPE Engineering Guide to Fire Exposure of Structural Elements. *Society of Fire Protection Engineers*, USA.

[16] NFPA (1917). Report of Committee on Fire-Resistive Construction, Proceedings of the *21st National Fire Protection Association Annual Meeting*, Boston, US, 391-413. Available via (www.nfpa.org).

[17] Magnusson S.E. and Thelandersson S. (1970). Temperature-time Curves of Complete Process of Fire Development – Theoretical Study of Wood Fuel Fires in Enclosed Spaces. *Acta Polytechnica Scandinavica, Civil Engineering and Building Series No. 65*, Stockholm, Sweden, 181 pp.

[18] CEN (2002). Eurocode 1: Actions on Structures – Parts 1-2: General Actions – Actions on Structures Exposed to Fire (EN 1991-1-2:2002). *European Committee for Standardization*, Brussels, Belgium, 62 pp.

[19] Corus (2006). Fire Resistance of Steel-framed Buildings, *Corus Construction and Industrial*, 40 pp.

[20] Stern-Gottfried J. and Rein G. (2012). Travelling Fires for Structural Design – Part I: Literature Review. *Fire Safety Journal*, 54, 74-85.

[21] Torero J.L., Majdalani A., Abecassis-Empis C., and Cowlard A. (2014). Revisiting the Compartment Fire. Proceedings of the *11th International Symposium on Fire Safety Science (IAFSS)*, Christchurch, New Zealand. (invited lecture)

[22] Bailey C.G., Burgees I.W., and Plank R.J. (1996). Computer Simulation of a Full-scale Structural Fire Test. *The Structural Engineer*, 74 (6), 93-100.

[23] Clifton G.C. (1996). Fire Models for Large Firecells. *New Zealand Heavy Engineering Research Association (HERA Report R4-83)*, Auckland, New Zealand.

[24] Stern-Gottfried J. and Rein G. (2012). Travelling Fires for Structural Design – Part II: Design Methodology. *Fire Safety Journal*, 54, 96-112.

[25] Ingberg S. (1928). Tests of the Severity of Building Fires. *National Fire Protection Association (NFPA) Quarterly*, 22, 43-61. Available via (www.nfpa.org).

[26] Kawagoe K. (1958). Fire Behaviour in Rooms. *Building Research Institute*, Japan, 76 pp.

[27] Butcher E.G. and Cooke G.M.E. (1969). Structural Steel and Fire. Proceedings of the *Conference on Steel in Architecture*, London, UK, 12 pp.

[28] Thomas P.H. (1970) The Fire Resistance Required to Survive a Burn Out (Fire Research Notes No. 901). *Fire Research Station*, London, UK, 32 pp.

[29] CEN (2012). Eurocode: Fire Resistance Tests – Part 1: General Requirements (EN 1363-1:2012). *European Committee for Standardization*, Brussels, Belgium, 56 pp.

[30] Incropera F.P. and DeWitt D.P. (2002), *Fundamentals of Heat and Mass Transfer*. Wiley & Sons, New York, NY, US.

[31] Torero J.L., Jowsey A., Usmani A., Lane B., and Lamont S. (2004). Structures in Fire: An Overview of the Boundary Condition. *Fire and Structures: The Implications of the World Trade Center Disaster*, The Royal Society of Edinburgh, Edinburgh, UK, 3-14.

[32] Lienau D. (1878). Fire Proof Construction. The American Architect and Building News, Vol. 3, 5-6.
Available via (babel.hathitrust.org/cgi/pt?id=njp.32101080160904;view=2up;seq=28).

[33] Rasbash D.J. (1974). New Variation On an Old Theme. *Inaugural lecture presented at The University of Edinburgh*, UK, 11 pp.

[34] Kendall J. (1912). *Fire Prevention and Fire Protection as Applied to Building Construction – A handbook of Theory and Practice*, John Wiley & Sons, NY, US.

[35] Miller R.P. and Stewart P.M. (1902). Making Buildings Safe: Fireproof Materials and Methods of Construction. *New York Tribune*, 19 October 1902. Available via (chroniclingamerica.loc.gov/lccn/sn83030214/1902-10-19/ed-1/seq-17/).

[36] Sachs E.O. (1903). Suggested Standard of Fire Resistance. Proceedings of the *International Fire Prevention Congress*, London, UK, 243-248.

[37] Welsch (1903). The Need for a Uniform Method of Testing the Fire Resistance of Building Materials. Proceedings of the *International Fire Prevention Congress*, London, UK, 249.

[38] Woolson I.H. (1904). For Fire Prevention. *New York Tribune*, 8 June 1904.

[39] NFPA (1918). Report of Committee on Fire-Resistive Construction, Proceedings of the *22nd National Fire Protection Association Annual Meeting*, Boston, US, 170-221. Available via (www.nfpa.org).

[40] ASTM (2012). Standard Test Methods for Fire Tests of Building Construction and Materials (ASTM E119). *American Society for Testing and Materials (ASTM)*, West Conshohocken, PA, United States, 34 pp.

[41] CEN (1999). Eurocode: Fire Resistance Tests – Part 2: Alternative and Additional Procedures (EN 1363-2:2012). *European Committee for Standardization*, Brussels,

Belgium, 20 pp. Available via (www.vie-publique.fr/documents-vp/circulaire_25-08-2000-1.pdf).

[42] MET (2000). Tunnel Safety in the National Road Network (in French), *Circulation of Inter-Ministerial Correspondence (N° 2000-63), Ministre de l'Equipement, des Transports et du Logement*, Paris, France, 53 pp. Available via (www.vie-publique.fr/documents-vp/circulaire_25-08-2000-1.pdf).

[43] RobK (2006). Guidelines for the Design of Concrete Infrastructure Works – Version 6 (in Dutch). *Ministerie van Infrastructuur en Milieu – Rijksoverheid (report RabK-6)*, The Hague, Netherlands, 45 pp. Available via (publicaties.minienm.nl/documenten/richtlijnen-voor-het-ontwerpen-van-betonnen-kunstwerken-robk-ver).

[44] FGSV (1985). Guidelines for Tunnel Equipment and Operation (in German), *Forschungsgesellschaft für Straßen- und Verkehrswesen (FGSV)*.

[45] Keough J.J. (1976). Design of Furnaces for Testing Fire Resistance of Structures. *Experimental Building Station*, Australia, 6 pp.

[46] Wickström U. (1986). A Proposal Regarding Temperature Measurements in Fire Test Furnaces. *Technical Report from the Nordtest Project 355-82*, 37 pp.

[47] Harmathy T.Z., Sultan M.A., and MacLaurin J.W. (1987). Comparison of Severity of Exposure in ASTM E 119 and IS0 834 Fire Resistance Tests. *ASTM Journal of Testing and Evaluation*, 15 (6), 371-375.

[48] CEN (2000). Eurocode: Fire Resistance Tests – Part 3: Verification of Furnace Performance (EN 1363-3:2000). *European Committee for Standardization*, Brussels, Belgium, 24 pp.

[49] FABIG (2014). Design Guidance for Hydrocarbon Fires. *The Steel Construction Institute (SCI) and Fire and Blast Information Group (FABIG) Technical Note 13*, Silwood Park, UK, 124 pp.

[50] Harmathy T.Z. (1981). The Fire Resistance and its Relation to Real-world Fires. *Fire and Materials*, 5 (3), 112-122.

[51] ISO (1995). Fire-resistance Tests – Elements of Building Construction – Part 1: General Requirements (ISO 834-1:1995). *International Organization for Standardization*, Geneva, Switzerland.

[52] Harmathy T.Z. (1969). Design of Fire Test Furnaces. *Fire Technology*, 5 (2), 140-150.

[53] Harmathy T.Z. and Mehaffey J.R. (1982). Normalized Heat Load: A Key Parameter in Fire Safety Design. *Fire and Materials*, 6 (1), 27-31.

[54] Cooke G.M.E. (1994). Can Harmonisation Of Fire Resistance Furnaces Be Achieved By Plate Thermometer Control? Proceedings of the *4th International Symposium on Fire Safety Science (IAFSS)*, Ontario, Canada, 1195-1207.

[55] Kruppa J. and Curtat M. (1995). Comments on Wickström's "The Plate Thermometer – A Simple Instrument for Reaching Harmonized Resistance Tests". *Fire Technology* (letter to editor), 31 (1), 84-90.

[56] Babrauskas V. and Williamson R.B. (1978). The Historical Basis of Fire Resistance Testing – Part II. *Fire Technology*, 14 (4), 304-316.

[57] Bressloff N., Rubini P., and Cox G. (1995). Computational Fluid Dynamics Modelling of a Fire Resistance Furnace. Proceedings of the *1st European Symposium on Fire Safety Science*, Zurich, Switzerland,13 pp.

[58] Harada K., Yabuki Y., and Terai T. (1997). A Theoretical Consideration On Heat Transfer In Fire Resistance Furnaces For Furnace Harmonization. Proceedings of the *5th International Symposium on Fire Safety Science (IAFSS)*, Melbourne, Australia, 1033-1044.

[59] Welch S. and Rubini P. (1997). Three-dimensional Simulation of a Fire-Resistance Furnace. Proceedings of the *5th International Symposium on Fire Safety Science (IAFSS)*, Melbourne, Australia, 1009-1020.

[60] Seigel L.G. (1970). Fire Test Standard in the Light of Fire Research. *Fire Test Performance – ASTM Special Technical Publication 464*, 57-67. Available via (www.astm.org).

[61] Kanury A.M. and Holve D.J. (1975). A Theoretical Analysis of the ASTM E-119 Standard Fire Test of Building Construction and Materials. *National Bureau of Standards*, Washington, DC, US, 152 pp.

[62] Torero J.L. (2014). Assessing the Performance of Concrete Structures in Fires. *Concrete in Australia – Concrete Institute of Australia*, 40 (3), 44-49.
Available via (www.concreteinstitute.com.au).

[63] Olsson S. (1993). Calibration of Fire Resistance Furnaces with Plate Thermometers (Report EUR 14555 EN), *Commission of the European Communities*, Luxembourg, 127 pp.

[64] Gross D. and Loftus J.J. (1963). Surface Flame Propagation on Cellulosic Materials Exposed to Thermal Radiation. *Journal of Research*, 67C (3), 252-258.

[65] Robertson A.F. (1982). Development of an improved radiant heat source for fire testing, *Fire and Materials*, 6 (2), 68-71.

[66] Anon T. (1986). Brand Verhalten von Stahl und Stahlverbund Konstructionen (Fire Behaviour of Steel and Composite Construction), *Verlag TUV Rheinland*, Cologne, Germany.

[67] Mowrer F.W. (1998). Window Breakage Induced by Exterior Fires. National Institute of Standards and Technology (NIST-GCR 98-751), 46 pp.

[68] Mell W.E. and Lawson J.R. (2000). Heat Transfer Model for Fire Fighter's Protective Clothing. Fire Technology, 36 (1), 39-68.

[69] Sakji S., Soize C., and Heck J.V. (2008). Probabilistic Uncertainty Modeling for Thermomechanical Analysis of Plasterboard Submitted to Fire Load. *Journal of Structural Engineering*, 134 (10), 1611-1618.

[70] Quarles S.L. and Sindelar M. (2011). Wildfire Ignition Resistant Home Design (WIRHD) Program: Full-scale Testing and Demonstration Final Report. *Technical Report for the National Technical Information Service*, US, 34 pp.

[71] ASTM (2013). Standard Test Method for Heat and Visible Smoke Release Rates for Materials and Products Using an Oxygen Consumption Calorimeter (ASTM E1354). American Society for Testing and Materials (ASTM), 20 pp.

[72] ISO (2002). Reaction-to-fire tests – Heat release, smoke production and mass loss rate – Part 1: Heat release rate (cone calorimeter method) (ISO 5660-1:2002). *International Organization for Standardization*, Geneva, Switzerland, 39 pp.

[73] ASTM (2002). Standard Test Methods for Measurement of Material Flammability Using a Fire Propagation Apparatus (FPA) (ASTM E2058). American Society for Testing and Materials (ASTM), 30 pp.

[74] ISO (2011). Reaction to fire tests – Measurement of material properties using a fire propagation apparatus (ISO 12136:2011). *International Organization for Standardization*, Geneva, Switzerland, 47 pp.

[75] Harmathy T.Z. and Lie T.T. (1970). Fire Test Standard in the Light of Fire Research. *Fire Test Performance – ASTM Special Technical Publication 464*, 85-97.

[76] Bøhm, B. (1978). Fire Resistance Tests and Differentiated Design Procedures – The Building Code: Aims and Means. *Fire Technology*, 14 (3), 239-246.

[77] Yabuki Y., Harada K. and Terai T. (1995). Heat Transfer in Fire Resistance Test Furnace with Particular References to Gas Radiation. Proceedings of the *2nd Asia-Oceania Symposium on Fire Science & Technology*, 262-273.

[78] Fromy P. and Curtat M.R. (2000). Application of a Zone Model to the Simulation of Heat Transfer in Fire Resistance Furnaces Piloted with Thermocouples or Plate Thermometers. Proceedings of the *6th International Symposium on Fire Safety Science (IAFSS)*, Poitiers, France, 531-542.

[79] Maluk C. (2014). Development and Application of a Novel Test Method for Studying the Fire Behaviour of CFRP Prestressed Concrete Structural Elements. PhD Thesis, *The University of Edinburgh*, UK, 473 pp.

[80] Kidd C.T. and Nelson C.G. (1995). How the Schmidt-Boelter Gage Really Works, Proceedings of the *41st International Instrumentation Symposium*, Research Triangle Park, NC, United States, 347–368.

[81] Filtz J.R., Lièvre M., Valin T., Hameury, J., Wetterlund I., Persson B., Andersson P., Jansson R., Lemaire T., Öhlin M., and Myllymäki J. (2002). Improving Heat Flux Meter Calibration for Fire Testing Laboratories (HFCAL). Technical report elaborated for the *Direction Générale des Affaires Economiques et Financières*, Brussels, France, 121 pp.

[82] ISO (2007). Fire tests – Calibration and Use of Heat Flux Meters – Part 4: Guidance on the Use of Heat Flux Meters in Fire Tests (ISO 14934-4:2007). *International Organization for Standardization*, Geneva, Switzerland, 30 pp.

[83] Pitts W.M., Murthy A.V., de Ris J.L., Filtz J.R., Nygård K., Smith D., and Wetterlund I. (2006). Round Robin Study of Total Heat Flux Gauge Calibration at Fire Laboratories. *Fire Safety Journal*, 41(6), 459-475.

[84] Maluk C., Bisby L., and Terrasi G. (2015). Effects of Polypropylene Fibre Type and Dose on the Propensity for Heat-Induced Concrete Spalling. *Engineering Structures*. (in press)

[85] Hulin T., Maluk C., Bisby L., Hodicky K., Schmidt J.W., and Stang H. (2015). Experimental Studies on the Fire Behaviour of High Performance Concrete Thin Plates. *Fire Technology*, 52(3), 683-705.

[86] Rickard I., Maluk C., Robert F., Bisby L., Deeny S., and Tessier C. (2015). Development of a Novel Small-scale Test Method to Investigate Heat-induced Spalling of Concrete Tunnel Linings. Proceedings of the *4th International Workshop on Concrete Spalling due to Fire Exposure*, Leipzig, Germany, 10 pp.

[87] Elliott A., Temple A., Maluk C., and Bisby L. (2014). Novel Testing to Study the Performance of Intumescent Coatings under Non-Standard Heating Regimes. Proceedings of the *11th International Symposium on Fire Safety Science (IAFSS)*, Canterbury, New Zealand, 14 pp.

[88] Bartlett A., Hadden R., Bisby L., and Law A. (2014). Analysis of Cross-laminated Timber Charring Rates Upon Exposure to Non-standard Heating Conditions. *Fire and Materials*, 2-4 February, San Francisco, USA.

[89] Brandon D., Maluk C., Ansell M.P., Harris R., Walker P., Bisby L., and Bregulla J. 2015. Fire Performance of Metal-Free Timber Connections. Construction Materials (Institution of Civil Engineers), 168(4), 173-186.

[90] Hidalgo-Medina J. (2015). Performance-based Methodology for the Fire Safe Design of Insulation Materials in Energy Efficient Buildings. PhD Thesis, *The University of Edinburgh*, UK, 429 pp.

[91] Arup Fire (2005). Fire Resistance of Concrete Enclosure – Work Package 1 and 2 (Rev B). *Elaborated for the Nuclear Safety Directorate of the Health and Safety Executive (HSE)*, London, UK, 36 pp.

[92] Hertz K.D. (1984). Heat-Induced Explosions of Dense Concrete. *Technical University of Denmark (Report No.166)*, Lyngby, Denmark, 20 pp

[93] Khoury G.A. (2008). Polypropylene Fibres in Heated Concrete – Part 2: Pressure Relief Mechanisms and Modelling Criteria. *Magazine of Concrete Research*, 60 (3), 189-204.

[94] CEN (2004). Eurocode 2: Design of Concrete Structures – Parts 1-1: General Rules and Rules for Buildings (EN 1992-1-1:2004). *European Committee for Standardization*, Brussels, Belgium, 230 pp.

[95] Bilodeau A., Kodur V.K.R., and Hoff G.C. (2004). Optimization of the Type and Amount of Polypropylene Fibres for Preventing the Spalling of Lightweight Concrete Subjected to Hydrocarbon Fire. Cement & Concrete Composites, 26 (2), 163-174.

[96] Terrasi G., Bisby L., Barbezat M., Affolter C., and Hugi, E. (2012). Fire Behavior of Thin CFRP Pretensioned High-Strength Concrete Slabs. *Journal of Composites for Construction*, 16 (4), 381–394.

[97] CEN (2010). Eurocode: Testing Fresh Concrete – Part 8: Self-compacting Concrete – Slump-flow Test (EN 12350-8:2010). *European Committee for Standardization*, Brussels, Belgium, 14 pp.